Highlights

- New experimental data of helium release in a scaled garage are obtained
- A CFD model is built and validated using the new helium data
- Three relations are studied for the similarity between hydrogen and helium leakage
- The accuracy of these relationships is assessed using the validated CFD model

Assessment of similarity relations using helium for prediction of hydrogen dispersion and safety in an enclosure

Jiaqing He[1,2], Erdem Kokgil[2], Liangzhu (Leon) Wang[2] and Hoi Dick Ng[1†]

[1]Department of Mechanical and Industrial Engineering
Concordia University, Montréal, Québec, H3G 1M8, Canada

[2]Department of Building, Civil and Environmental Engineering
Concordia University, Montréal, Québec, H3G 1M8, Canada

[†]Corresponding Author
Department of Mechanical and Industrial Engineering
Concordia University
1455 de Maisonneuve Blvd. West
Montréal, Québec, H3G 1M8, Canada
Tel.: +1 (514) 848-2424 (ext. 3177)
Fax: +1 (514) 848-3175
E-mail: hoing@encs.concordia.ca

Revised manuscript submitted to the *International Journal of Hydrogen Energy*

June 2016

Assessment of similarity relations using helium for prediction of hydrogen dispersion and safety in an enclosure

Jiaqing He, Erdem Kokgil, Liangzhu (Leon) Wang and Hoi Dick Ng

Abstract

The ability to predict the concentration of hydrogen in a partially confined space is significant to the safe use of hydrogen-related products such as fuel cell vehicles. Hydrogen release and subsequent dispersion are frequently investigated using commercially-available computational fluid dynamic (CFD) models once those are calibrated with available experimental data. Due to the explosion safety concerns of using hydrogen, accidental scenarios are often replicated with helium as a hydrogen simulant in experiments. Currently, there is no validated, theoretical analogy to correlate the helium data in order to predict the spatial and temporal distribution of hydrogen in the enclosure. The aim of this paper is to assess different theoretical relationships for the similarity between hydrogen and helium leakage in an enclosure. Experiments were first carried out to obtain measured data with helium leakage in a set of scenarios and to validate the present CFD model. Three methods, namely equal volumetric flow rate, equal buoyancy and a newly proposed correlation derived from equal concentration, were employed to determine the equivalent hydrogen release rate, using which the validated CFD model was then used, with the physical property values for hydrogen, to stimulate hydrogen dispersion as compared to that of helium. The accuracy of these different methods at different stage of release and location is discussed. The present result thus provides a guide when using helium experiment to validate hydrogen simulation in different scenarios, which is of importance to the investigation of hydrogen safety.

Keywords: Hydrogen safety; fuel cells; helium; hydrogen leakage; CFD; correlation.

Nomenclature

b	Plume radius [m]
B	Buoyancy flux [m^4/s^3]
C	Volumetric concentration
g	Gravity [m/s^2]
$\dot{m}$	Mass flow rate [kg/s]
n	correlation exponent
Q	Volumetric flow rates [m^3/s]
u	Plume vertical velocity [m/s]
v	Air entrainment velocity [m/s]
z	Height [m]

Greek letters

α	Entrainment ratio
ρ	Density [kg/m^3]

1. Introduction

Hydrogen is considered as one of the leading fuels for a renewable and environment friendly energy carrier in the near future [1-6]. In particular, fuel cells using hydrogen present significant advantage in reducing carbon emissions generated by transportation systems and have higher efficiency when compared with traditional fossil fuels [7-10]. However, the high-pressure storage and use of hydrogen pose unique challenges due to its ease of leaking, low-energy ignition, a wide range of combustible fuel-air mixtures, high buoyancy and diffusion rate in air [11-16]. As such, the ability to predict the behavior of leaked hydrogen in an enclosure under different scenarios is of great importance.

An extensive wealth of studies on hydrogen release and dispersion can be found in the literature. For example, fundamental investigations on hydrogen dispersion and explosion predictions in simple geometries, like an enclosure or tunnel, have been carried out experimentally (e.g., [17-23], etc.) and with Computational Fluid Dynamics (CFD) (e.g., [24-36], etc.). Current research efforts, both experimental and computational, are starting more toward engineering aspects of real hydrogen vehicles and refueling station systems in practical environment and scenarios [37-45]. Although CFD tools have the potential to predict hydrogen dispersion and explosion with reasonable accuracy, those often required inter-comparison between different models, extensive calibration and validation efforts together with experiments [31-35]. Due to safety concerns, large-scale experimental data of hydrogen release remain scarce [42-46]. Hence, most of current hydrogen experiments against which CFD models were validated, are limited to small volumes or scaled experiments in simple enclosure geometries.

To alleviate any concern of accidental combustion while obtaining large-scale experimental data for CFD model calibration, helium was considered as a hydrogen stimulant due to the

similar low densities of the two gases [47-51]. Swain et al. [47-49] used helium to simulate leakage scenario experimentally and to predict using a calibrated CFD model with helium data the spatial and temporal distribution of leaking hydrogen gas in equivalent accidental settings. The studies conducted by Swain et al. [47-49] formed the methodology referred to as the hydrogen risk assessment method (HRAM). This method consists of the following four steps: 1) Simulate the leakage scenario with helium; 2) calibrate a CFD model of the leakage scenario using the helium experimental data; 3) predict the distribution of hydrogen using the calibrated CFD model; and 4) assess the risk from the numerically simulated concentration of hydrogen leakage [49].

Helium is also used in a number of recent studies as a surrogate gas to analyze the dispersion behavior of hydrogen in a ¼-scale and a realistic full-scale residential garage parked with a hydrogen-fuelled vehicle [50-53]. The effects of injected volume, location and characteristics of leakage source (i.e., jet or plume) within the enclosure on the dispersion and mixing dynamics are investigated. The presence of ventilation is also considered using different combination of vent size, number and location.

For the aforementioned studies, the similarity is often assumed with helium released in an equal volumetric flow rate as with hydrogen. However, it has been found that there exists a difference between hydrogen and helium concentrations before the plume becomes stable, particularly during the initial release of the gases [47, 48]. Currently, the equivalent behavior between the two gases only relies on numerical or experimental results, and the similarity is not backed up by a theoretical correlation. Therefore, the objective of the present study is to report an analysis of helium and hydrogen similarity for the commonly used method of equal volumetric flow rate, and two new methods based on the theoretical plume characteristics, and to

compare the three methods by measurements and CFD simulations. Experiments using time-resolved measurements of helium concentrations at multiple heights in a sub-scaled garage model during the releases phase were conducted to obtain helium concentration data at a set of initial conditions. These experimental data were used to validate the CFD model in the present study. The validated CFD model was then used, with the physical property values for hydrogen, to simulate hydrogen release and dispersion while using the three different methods to determine the equivalent hydrogen release rate as compared to that of helium. A numerical resolution study was also presented to ensure the convergence of the numerical results using the chosen mesh size for the simulations.

2. Theory

From the previous work by Swain et al. [49] where the hydrogen risk assessment method (HRAM) is introduced, it shows that, in simple geometric enclosures, helium can be used to simulate leakages of hydrogen and to predict the hydrogen concentrations near the ceiling. The method to assess the risk of hydrogen leakage relies on a CFD model calibrated by the data from helium experiments. The similarity between hydrogen and helium is obtained based on $Q_{H2} = Q_{He,}$ where Q_{H2} and Q_{He} are volumetric flow rates of hydrogen and helium, in m^3/s, respectively. Most current studies using helium as a surrogate to validate hydrogen simulation models are also formulated by assuming the same volumetric flow rate of both gases. Nevertheless, Swain et al. [48] observed that, before the plume becomes stable during the development stage, the helium concentration can be significantly different from that of hydrogen using the aforementioned analogy.

In order to use helium accurately as a surrogate gas for hydrogen, it is necessary to assess the similarity between the hydrogen and helium plumes. Inspired by the ideal plume theory in the field of fire science [54], the ideal plume models of hydrogen and helium can be developed as shown in Fig. 1. Similar to that of a fire plume, the buoyancy flux of a buoyant gaseous plume, B in m^4/s^3, can be defined by:

$$B = gQ_{gas}\left(\frac{\rho_{air} - \rho_{gas}}{\rho_{air}}\right) \tag{1}$$

where ρ_{air} is the surrounding air density in kg/m^3, g is the acceleration of gravity, in m/s^2, and Q_{gas} is the volumetric flow rate of the plume, in m^3/s. In this study the temperature is assumed to be constant in the plume and in the ambient air and thus, the difference of density is caused by a scale factor, which is a function of the height z. The volumetric flow of the gas Q_{gas} is also kept constant. The volumetric concentration, C, is then given by:

$$C = \frac{Q_{gas}}{Q_{plume}} = \frac{Q_{gas}}{\pi b^2 u} \tag{2}$$

b is the radius of the plume, u is the upward gas velocity. The density and the mass flow rate of the plume are thus:

$$\rho_{plume} = C\rho_{gas} + (1-C)\rho_{air} = \rho_{air} + \frac{Q_{gas}}{\pi b^2 u}\left(\rho_{gas} - \rho_{air}\right) \tag{3}$$

$$\dot{m}_{plume} = Q_{plume}\rho_{plume} = \pi b^2 u \rho_{plume} \tag{4}$$

The ambient air is assumed to entrain at a rate proportional to the plume velocity u, i.e., $v = \alpha \cdot u$, where α is referred to as the entrainment ratio. By equating the rate of mass change over the height dz and the rate of air entrainment through the sides of dz satisfying the conservation of mass, it yields:

$$\frac{d\dot{m}_{plume}}{dz} = \frac{d(\pi b^2 u \rho_{plume})}{dz} = \frac{2\pi b u \alpha \rho_{air} dz}{dz}$$

$$\frac{d(b^2 u \rho_{plume})}{dz} = 2bu\alpha\rho_{air} \tag{5}$$

Similarly, by equating the rate of momentum change over height dz and the differential buoyancy force acting on the mass within height dz based on the conservation of momentum, the following expression is obtained:

$$\frac{d(\dot{m}_{plume} u)}{dz} = \frac{dF}{dz}$$

$$\frac{d(\pi b^2 u^2 \rho_{plume})}{dz} = g(\rho_{air} - \rho_{plume})\pi b^2 \tag{6}$$

Solving the two combined differential equations above, it gives:

$$C(z) = \frac{Q_{gas}}{Q_{plume}} = \frac{Q_{gas}}{\pi b^2 u} = \frac{Q_{gas}}{\pi \frac{36}{25}\alpha^2 \left[\frac{25 B_{gas}}{48\pi\alpha^2}\right]^{1/3} z^{5/3}} \tag{7}$$

In order to obtain the same concentration level for both hydrogen and helium,

$$C_{H2}(z) = C_{He}(z)$$

$$\frac{Q_{H2}}{\pi \frac{36}{25}\alpha^2 \left[\frac{25 g Q_{H2}\left(\frac{\rho_{air} - \rho_{H2}}{\rho_{air}}\right)}{48\pi\alpha^2}\right]^{1/3} z^{5/3}} = \frac{Q_{He}}{\pi \frac{36}{25}\alpha^2 \left[\frac{25 g Q_{He}\left(\frac{\rho_{air} - \rho_{He}}{\rho_{air}}\right)}{48\pi\alpha^2}\right]^{1/3} z^{5/3}} \tag{8}$$

After some mathematical manipulation, the following relationship can be obtained:

$$Q_{He} = Q_{H2}\sqrt{\frac{(\rho_{air} - \rho_{He})}{(\rho_{air} - \rho_{H2})}} \tag{9}$$

Using the above correlation, for any given hydrogen volumetric flow rate, the helium volumetric flow rate can be calculated which gives the exact concentration level as hydrogen, or vice-versa.

For fire science applications, it is common to maintain a same buoyancy flux to ensure the dynamical similarity of plumes [55-57]. Similarly, it is also possible to come up with another correlation based on the equal buoyancy flux of the two gases:

$$B_{He} = B_{H2} \tag{10}$$

and it gives:

$$Q_{He} = Q_{H2} \frac{\left(\rho_{air} - \rho_{He}\right)}{\left(\rho_{air} - \rho_{H2}\right)} \tag{11}$$

Combine the above two correlations into one, a generalized expression can be obtained as:

$$Q_{He} = Q_{H2} \left[\frac{\left(\rho_{air} - \rho_{He}\right)}{\left(\rho_{air} - \rho_{H2}\right)} \right]^{n} \tag{12}$$

When n = 1/2, the correlation is based on equal concentration as derived in this section (Method A); For the n = 0, the above equation reduces to the equal volumetric flow rate (Method B or equivalently the HRAM method); and finally, the equal buoyancy model is yielded with n = 1 (Method C).

3. Numerical Simulation

3.1 Numerical modeling of reduced scale experiments with helium

In this study, the CFD simulations were divided into two stages. The chosen CFD model was first validated with experimental data of helium release in the scaled enclosure, see Fig. 2a. Simulations of hydrogen dispersion were then conducted using the validated CFD model and the results were used to assess the similarity models described in Sec. 2.

For the experiment, a 1.5 m × 1.5 m × 0.75 m with 0.6-cm-thick chamber made of Plexiglas was built, representing a 1:4 scaled two-car residential garage. An injector was used to release the helium into the chamber. The injector was 12.5 cm tall and the inlet size was 36 mm × 36 mm. A uniform room temperature of 21°C is expected to maintain at the exit section. A mass flow controller adjusted the helium flow at 15 L/min (- a typical hydrogen leakage rate for hydrogen storage tanks is 1 to 15 L/min). Several small vents were chosen to provide minimum ventilation requirements for residential garages, of 3 air changes per hour (ACH) [58]. The vents consist of single 2.6-cm-square openings at the center of the ceiling and at the top of the side faces. For the case of forced ventilation, the boundary condition in the ceiling vent was changed to a ventilation fan with 4.2 CFM (from the ASHRAE standard [58]). Helium concentrations were measured with eight sensors, at two horizontal locations (i.e., one at 40 cm from the side and the front, and the other at the floor center). Sensors 1 to 4 and sensors A to D were located inside and outside the plume, respectively. Each set of sensors were mounted 0.4, 0.5, 0.6 and 0.65 m above the floor, see Figs. 2b to 2d.

The commercial software ANSYS FLUENT [59] was used in this study for all simulation cases. The geometrical model utilized within the CFD is equivalent to that of the present reduced, scaled experiment with helium, as shown in Figs. 2b and 2c. A finite volume scheme with 2nd order accuracy was used to discretize the governing Navier-Stokes equations. A Large Eddy Simulation (LES) was applied as the turbulence model, and the PISO-SIMPLE (PIMPLE) algorithm with a time step size Δt of $4 \times 10^{-7} \sim 5 \times 10^{-7}$ for obtaining a stable solution to the discretizing equations [59-61]. All the numerical simulations were performed using the computer cluster available at the High Performance Computing Virtual Laboratory (HPCVL) managed by Compute Canada [62]. The simulations were performed using similar initial conditions as in the

experiment with a leak source located close to the floor in the garage. The leak area was 3.15 cm × 3.15 cm and the mass flow rate of the leak was 4.178×10^{-5} kg/s. Both the initial temperature of released helium and air temperature in the chamber were set equal to 297 K and initial pressure to 101 kPa. For the ceiling vent a pressure outlet boundary condition was used; while for side wall vent velocity inlet was used. The gas injection was modeled using a mass flow inlet boundary condition. A structured grid made of rectangular cells was used for meshing. Unless specified, the mesh size varies from 0.004 m close to the injector to a maximum value of 0.016 m. 484166 grid cells in total were contained in the computational model. A resolution study was indeed carried out and found that an increase in the current grid resolution has only a negligible effect on the concentration levels. Figure 3 shows the test results measured by sensors 1 and 4 inside the plume, and by sensors A and D for the layer outside the plume with three different mesh resolutions. It is found that an increase of the total mesh number by 10%, i.e., from 484166 to 523580 grid cells, results in a percentage difference less than 1% in the overall change of helium concentrations.

Figure 4 compares the evolution of helium concentration obtained from both the experimental measurement (given by discrete points) and CFD numerical simulation (represented by solid lines). Simulation time for this validation case lasts for 2,700 s. Overall, both results agree reasonably well with each other. The average percentage difference of the simulation results to experiment data for all sensors is 7.6%. Both results also show that the sensors inside the plume (Sensors 1 and 4) records accordingly higher concentrations than those obtained for sensors A-D in the layer region outside the plume.

3.2 Simulations of hydrogen leakage

The same CFD model validated in the above section is used to simulate the hydrogen dispersion in the same computational setting, with the physical property values for hydrogen instead of those for helium. To evoke the similarity, the equivalent hydrogen volumetric flow rate is determined using Eq. 12 with different n, giving the various correlation based on the newly proposed correlation obtained with equal concentration, equal volume flow rate and equal buoyancy with values of 15.6 L/min, 15.0 L/min and 13.88 L/min, respectively.

Figures 5 and 6 compare the numerical results for the evolution of helium and hydrogen concentrations, obtained based on the three similarity models. It is found that there is noticeable difference in the results obtained at different regions, i.e., inside the gas plume or outside the plume. Figure 5 shows the concentration results measured by the sensors 1 and 4 inside the plume which represents the high risk domain in hydrogen leakage. A large flow fluctuation also resulted inside the plume as shown in Fig. 5. In all cases, the graphs show that hydrogen has a similar tendency with helium with small difference. By defining the percentage difference as: $(C(\mathrm{He}) - C(\mathrm{H_2}))/C(\mathrm{He}) \times 100\%$ for a quantitative comparison, it is found that the time-averaged percentage differences from all sensors measurement for Method A, B and C are 4.4%, 5.5% and 6.5%, respectively (see also Table 1). The concentration levels outside the plume are presented in Fig. 6, and the results show less fluctuation than those in Fig. 5. Method B brings overall the minimum time-averaged percentage difference of 1.8%. In all cases, the average percentage differences obtained from the different methods are not pronounced, particularly if various uncertainties in the simulation (e.g., physical model, grid resolution, etc.) are taken into account. Hence, it is suggested that all three methods can be used when the region of interest is that inside the plume and for long time evolution at different layers outside the plume.

If the early stage of the release (i.e., less than 100 s) is of particular interest, however, Methods A and B might lead to a noticeable discrepancy. This result is indeed consistent with the finding by Swain et al. [48]. It is worth noting that based on the buoyancy effect Method C shows better similarity in the early stage of release (e.g., before 100 s) as shown in Fig. 7, except the measurement from the sensor D where the dispersion is influenced significantly by the near outlet located at the ceiling. Figure 7 also shows bumps in the initial stage of dispersion. At the very early instant, an increase of dispersed gas concentration accumulating in the ceiling is recorded by the sensors located at lower heights. As the surrounding air flows in through the outlet at the sidewall, a decrease in the gas concentration is resulted due to the air entrainment and leading to the appearance of these bumpy behaviors of the results.

From the plume model [54, 55], buoyancy is the main controlling parameter on the velocity when considering the gas plume,

$$u(z) = \left[\frac{25B_{gas}}{48\pi\alpha^2}\right]^{\frac{1}{3}} z^{-\frac{1}{3}} \tag{13}$$

It is worth noting that from the general transport equation, the gas release into the chamber is driven by both convection and diffusion mechanism [63]. From Eq. (13), equal buoyancy gives equal velocity which brings the same value of convection, while the value of diffusion is different. At the initial stage, the dispersion is driven mainly by convection. When the gas continuously diffuses into the chamber and accumulates at the upper layer leading to higher concentration gradient, the effect of diffusion will start to play a dominant role at later dispersion evolution. Method C which is formulated based on the equal buoyancy between helium and hydrogen plumes give a more similar plume shape in the initial release and therefore, as shown in Fig. 7, has the better accuracy in the initial stage when the dispersion is convection-dominated.

A parametric study using different configurations by changing the injection height and volumetric flow rate was also performed to explore the accuracy of the three methods at the early stage of release from 0 to about 100 s. It is indeed found that Method C always brings the least difference compared with the simulant (i.e., helium). For completeness, Figs. 8 and 9 present the results of these various parametric configurations obtained using the Method C to illustrate its accuracy at the early stage of release from 0 - 100 s.

In the case with the inclusion of the mechanically driven flow, we consider the result in the outside layer region due to the significant fluctuation inside the plume as showed in Fig. 10, preventing any meaningful comparison. Figure 11 compares the simulation results obtained based on Method A, B and C with helium in the outside layer. It can be observed that Method B presents the best correlation in Fig. 11 over the whole time interval from 0 to 2,700 s with a time-averaged percentage difference of 1.7% as compared to 11.3% and 7.0% determined for Method A and C, respectively. In the early stage, there is no huge difference for the reason that the ventilation fan weakens the plume effect, see Fig. 12. It is worth noting that the plume shape becomes stable at a very short time. As a result, the improvement by using Method C is not as good as that in the case of natural ventilation.

4. Concluding Remarks

In the literature, helium is often used in experiments as a surrogate to stimulate hydrogen dispersion. In this work, three different relationships for the similarity between hydrogen and helium are reported and assessed using numerical simulations. Sub-scaled experiments measuring the helium concentration were used to validate the present CFD model. The same CFD model was then run with the physical property values for hydrogen instead of those for

helium. The three correlations linking the helium with hydrogen based on equal concentration, equal volume flow rate and buoyancy were compared in the long-time release phase, early stage of release and the scenario with mechanical ventilation. If considering the overall time-averaged percentage difference inside the plume, the three methods give results close to each other. In the layer outside the plume, using the method of equal volumetric flow rate with helium gives the best overall results for the long-time release evolution. However, if the very early stage of release is of particular concern, the method of equal buoyancy (Method C) can improve the accuracy in multiple scenarios. While for the case of mechanical ventilation, the commonly used method (i.e., Method B) based on equal volumetric flow rate generally gives a reasonable similarity over the span of the release and at different regions. In this work, a detailed numerical investigation was conducted to highlight various possible similarity correlations to translate helium experiment into hydrogen simulation in different scenarios. The present results thus help to verify numerical approach in the study of hydrogen safety and the use of helium data for hydrogen dispersion analysis.

Acknowledgment

This work is supported by the Fonds de recherche du Québec – Nature et technologies (FRQNT): Projet de recherche en équipe for the project: “Safety analysis related to hydrogen leaks from fuel cell systems in residential areas” (#2015-PR-182638) led by L.L. Wang.

References

[1] Züttel A. Hydrogen: the future energy carrier. Phil Trans Roy Soc A 2010; 368:3329-3342.

[2] Schlapbach L. Technology: Hydrogen-fuelled vehicles. Nature 2009; 460:809-811.

[3] Balat M. Potential importance of hydrogen as a future solution to environmental and transportation problems. Int J Hydrogen Energy 2008; 33(15):4013-4029.

[4] Dodds P, Staffell I, Hawkes AD, Li F, Grünewald P, McDowall, W, Ekins, P. Hydrogen and fuel cell technologies for heating: A review. Int J Hydrogen Energy 2015; 40(5):2065-2083.

[5] Elam CC, Padro CEG, Sandrock G, Luzzi A, Lindblad P, Hagen EF. Realizing the hydrogen future: the International Energy Agency's efforts to advance hydrogen energy technologies. Int J Hydrogen Energy 2003; 28:601–607.

[6] Cipriani G, di Dio V, Genduso F, La Cascia D, Liga R, Miceli R, Galluzzo GR. Perspective on hydrogen energy carrier and its automotive applications. Int J Hydrogen Energy 2014; 39(16):8482-8494.

[7] Ogden JM, Steinbugler MM, Kreutz T. A comparison of hydrogen, methanol and gasoline as fuels for fuel cell vehicles: implications for vehicle design and infrastructure development. J Power Sources 1999; 79:143-168.

[8] Jacobson MZ, Colella WG, Golden DM. Cleaning the air and improving health with hydrogen fuel-cell vehicles. Science 2005; 308(5730):1901-1905.

[9] St-Pierre J, Wilkinson DP. Fuel cells: A new, efficient and cleaner power source. AlChe J 2001; 47(7):1482-1486.

[10] Momirlan M, Veziroglu TN. The properties of hydrogen as fuel tomorrow in sustainable energy system for a cleaner planet. Int J Hydrogen Energy 2005; 20(7):795-802.

[11] Ng HD, Lee JHS. Comments on explosion problems for hydrogen safety. J Loss Prev Proc Ind 2008; 21:136-146.

[12] Markert F, Nielsen SK, Paulsen JL, Andersen V. Safety aspects of future infrastructure scenarios with hydrogen refueling stations. Int J Hydrogen Energy 2007; 32(13):2227-2234.

[13] Najjar YSH. Hydrogen safety: The road toward green technology. Int J Hydrogen Energy 2013; 38(25):10716-10728.

[14] Reider R, Edeskuty FJ. Hydrogen safety problems. Int J Hydrogen Energy 1979; 4(1):41-45.

[15] DeLuchi MA. Hydrogen vehicles: an evaluation of fuel storage, performance, safety, environmental impacts, and cost. Int J Hydrogen Energy 1989; 14(2):81-130.

[16] Zheng J, Liu X, Xu P, Liu P, Zhao Y, Yang J. Development of high pressure gaseous hydrogen storage technologies. Int J Hydrogen Energy 2012; 37(1):1048-1057.

[17] Swain MR, Shriber J. Swain MN. Comparison of hydrogen, natural gas, liquid petroleum gas and gasoline leakage in a residential garage. Energy Fuel 1998; (12)(1):83-89.

[18] Friedrich A, Veser A, Stem G, Kotchourko N. Hyper experiments on catastrophic hydrogen releases inside a fuel cell enclosure. Int J Hydrogen Energy 2011; 36(3):2678-87.

[19] Houf W, Schefer R. Analytical and experimental investigation of small-scale unintended releases of hydrogen. Int J Hydrogen Energy 2008; 33:1435-1444.

[20] Petukhov VA, Naboko IM, Fortov VE. Explosion hazard of hydrogen-air mixtures in the large volumes. Int J Hydrogen Energy 2009; 34(14):5924-5931.

[21] Sommersel OK, Bjerketvedt D, Vaagsaether K, Fannelop TK. Experiments with release and ignition of hydrogen gas in a 3-m long channel. Int J Hydrogen Energy 2009; 34:5869-5874.

[22] Merilo EG, Groethe MA, Colton JD, Chiba S. Experimental study of hydrogen release accidents in a vehicle garage. Int J Hydrogen Energy 2011; 36:2436-2444

[23] Houf WG, Evans GH, Ekoto IW, Merilo EG, Groethe MA. Hydrogen fuel-cell forklift vehicle releases in enclosed space. Int J Hydrogen Energy 2013; 38:8179-8189.

[24] Kim E, Park J, Cho JH, Moon I. Simulation of hydrogen leak and explosion for the safety design of hydrogen fueling station in Korea. Int J Hydrogen Energy 2013; 38(3):1737-1743.

[25] Salva JA, Tapia E, Iranzo A, Pino FJ, Cabrera J, Rosa F. Safety study of a hydrogen leak in a fuel cell vehicle using computational fluid dynamics. Int J Hydrogen Energy 2012; 37(6): 5299-5306.

[26] Matsuura K, Kanayama H, Tsukikawa H, Inoue M. Numerical simulation of leaking hydrogen dispersion behavior in a partially open space. Int J Hydrogen Energy 2009; (33)(1):240-247.

[27] Prasad K, Pitts WM, Yang JC. Effect of wind and buoyancy on hydrogen release and dispersion in a compartment with vents at multiple levels. Int J Hydrogen Energy 2010; 35(17):9218-9231.

[28] Prasad K, Pitts WM, Yang JC. A numerical study of the release and dispersion of a buoyant gas in partially confined spaces. Int J Hydrogen Energy 2011; 36(8):5200-5210.

[29] Middha P, Hansen OR. CFD simulation study to investigate the risk from hydrogen vehicles in tunnels. Int J Hydrogen Energy 2009; 34(14):5875-5886

[30] Hajji Y, Bouteraa M, ELCafsi A, Belghith A, Bournot P, Kallel F. Numerical study of hydrogen release accidents in a residential garage. Int J Hydrogen Energy 2015; 40(31):9747-9759.

[31] Baraldi D, Kotchourkob A, Lelyakin A, Yanez J, Middha P, Hnasen OR, et al. An inter-comparison exercise on CFD model capabilities to simulate hydrogen deflagrations in a tunnel. Int J Hydrogen Energy 2009; 34(18):7862-7872.

[32] Gallego E, Migoya E, Martín-Valdepeñas JM, Crespo A, García J, Venetsanos A, Papanikolaou E, Kumar S, Studer E, Dagba Y, Jordan T, Jahn W, Høiset S, Makarov D, Piechna J. An inter-comparison exercise on the capabilities of CFD models to predict distribution and mixing of H_2 in a closed vessel. Int J Hydrogen Energy 2007; 32:2235-2245.

[33] Venetsanos A, Papanikolaou E, Delichatsios M, García J, Hansen OR, Heitsch M, Huser A, Jahn W, Jordan T, Lacome J-M, Ledin HS, Makarov D, Middha P, Studer E, Tchouvelev AV, Teodorczyk A, Verbecke F, Van der Voort MM. An inter-comparison exercise on the

capabilities of CFD models to predict the short and long term distribution and mixing of hydrogen in a garage. Int J Hydrogen Energy 2009; 34(14):5912-5923.

[34] Middha P, Hansen OR, Storvik IE. Validation of CFD model for hydrogen dispersion. J Loss Prev Proc Ind 2009; 22(6):1034-1038.

[35] Middha P, Hansen OR. Using computational fluid dynamics as a tool for hydrogen safety studies. J Loss Prev Proc Ind 2009; 22(3):295-302.

[36] Wilkening H, Baraldi D. CFD modelling of accidental hydrogen release from pipelines. Int J Hydrogen Energy 2007; 32(13):2206-2215.

[37] Makarov D, Verbecke F, Molkov V, Roe O, Skotenne M, Kotchourko A, Lelyakin A, Yanez J, Hansen O, Middha P, Ledin S, Baraldi D, Heitsch M, Efimenko A, Gavrikov A. An inter-comparison exercise on CFD model capabilities to predict a hydrogen explosion in a simulated vehicle refueling environment. Int J Hydrogen Energy 2009; 34(6):2800-2814.

[38] Venetsanos AG, Baraldi D, Adams P, Heggem PS, Wilkening H. CFD modelling of hydrogen release, dispersion and combustion for automotive scenarios. J Loss Prev Proc Indust 2008; 21(2)162-184.

[39] Venetsanos AG, Huld T, Adams P, Bartzis JG. Source, dispersion and combustion modelling of an accidental release of hydrogen in an urban environment. J Hazard Mater 2003; 105(1):1-25.

[40] Wen JX, Madhav Rao VC, Tam VHY. Numerical study of hydrogen explosions in a refueling environment and in a model storage room. Int J Hydrogen Energy 2010; 35(1):385-394.

[41] Kikukawa S. Consequence analysis and safety verification of hydrogen fueling stations using CFD simulation. Int J Hydrogen Energy 2008; 33(4):1425-1434.

[42] Watanabe S, Tamura Y, Suzuki J. The new facility for hydrogen and fuel cell vehicle safety evaluation. Int J Hydrogen Energy 2007; 32(13):2154-2161.

[43] Tanaka T, Azuma T, Evans JA, Cronin PM, Johnson DM, Cleaver RP. Experimental study on hydrogen explosions in a full-scale hydrogen filling station model. Int J Hydrogen Energy 2007; 32(13):2162-2170.

[44] Shirvill LC, Roberts TA, Royle M, Willoughby DB, Gautier T. Safety studies on high-pressure hydrogen vehicle refueling stations: Release into a simulated high-pressure dispensing area. Int J Hydrogen Energy 2012; 37(8)6949-6964.

[45] Reinecke EA, Huebert T, Tkatschenko I, Kessler A, Kuznetsov M, Wilkins M, Hedley D, Azkarate I, Proust C, Acosta-Iborra B, Gavrikov B, De Bruijn PCJ, Marangon A, Teodorczyk A, Grafwallner A. Integration of experimental facilities: A joint effort for establishing a common knowledge base in experimental work on hydrogen safety. Int J Hydrogen Energy 2011; 26(3):2700-2710.

[46] Pitts WM, Yang JC, Blais M, Joyce A. Dispersion and burning behavior of hydrogen released in a full-scale residential garage in the presence and absence of conventional automobile. Int J Hydrogen Energy 2012; 37:17457-17469.

[47] Swain MR, Filoso P, Grilliot ES, Swain MN, Hydrogen leakage into simple geometric enclosures. Int J Hydrogen Energy 2002; 28(2):229-248.

[48] Swain MR., Grilliot, E. S., & Swain, M. N. (1999). Experimental verification of a hydrogen risk assessment method. Chem Health Safety 1999; 6(3):28-32.

[49] Swain MR, Grilliot ES, Swain MN. The application of a hydrogen risk assessment method to vented spaces. In: Grégoire Padró CE, Lau F. (Eds.), Advances in Hydrogen Energy. Springer, NY, 2002.

[50] Pitts WM, Yang JC, Fernandez MG. Helium dispersion following release in a ¼-scale two-car residential garage. Int J Hydrogen Energy 2012; 37:5286-5298.

[51] Gupta S, Brinster J, Studer E, Tkatschenko I. Hydrogen related risks within a private garage: concentration measurements in a realistic full scale experimental facility. Int J Hydrogen Energy 2009; 34:5592-5603.

[52] Cariteau B, Brinster J, Studer E, Tkatschenko I, Joncquet G. Experimental results on the dispersion of bouyant gas in a full scale garage from a complex source. Int J Hydrogen Energy 2011; 36(3):2489-2496.

[53] Prasad K, Pitts WM, Fernandez M, Yang JC. Natural and forced ventilation of buoyant gas released in a full-scale garage: Comparison of model predictions and experimental data. Int J Hydrogen Energy 2012; 37(22):17436-17445.

[54] Karlsson B, Quintiere J. Enclosure Fire Dynamics. CRC Press, Florida, 1999.

[55] Kokgil E. Using Helium as Hydrogen Surrogate for Safety Analysis Related to Hydrogen Leaks from Residential Fuel Cell Systems. Masters thesis, Concordia University, Montreal, Canada, 2015.

[56] Wang L, Zhao G. Numerical study on smoke movement driven by pure helium in atria. Fire Safety J 2013; 61:45-53.

[57] Zhao G, Wang L. Using helium smoke as a surrogate of fire smoke for the study of atrium smoke filling. J. Fire Sci. 2014; 32(5):431-447.

[58] ANSI/ASHRAE. Standard 62.1 Ventilation for Acceptable Indoor Air Quality, 2013.

[59] ANSYS FLUENT 14.5 User's Guide. ANSYS. 2009.

[60] Barton IE, Comparison of SIMPLE- and PISO-type algorithms for transient flows. Int J Numer Meth Fluids 1998; 26:459-483.

[61] Ferziger J, Peric M Computational Methods for Fluid Dynamics, 2nd ed. Springer-Verlag, Berlin, 1999.

[62] High Performance Computing Virtual Laboratory. (2015). Retrieved from http://www.hpcvl.org/

[63] Patankar SV. Numerical Heat Transfer and Fluid Flow. Hemisphere, Washington DC, 1980.

List of Tables

List of Figures

Figure 11. Comparison of hydrogen concentration plume (solid lines) at the layer outside the plume with helium results (dashed line) based on a) Method A; b) Method B; and c) Method C with forced ventilation

Figure 12. Comparison of hydrogen concentration (solid lines) at the layer outside the plume with helium results (dashed line) for the early release stage from 0 to 270 s based on a) Method A; b) Method B; and c) Method C with forced ventilation

Table

	Sensor 1, 2, 3 and 4 (inside plume)	Sensor A, B, C, D (outside layer)
Method A	4.4%	4.1%
Method B	5.5%	1.8%
Method C	6.5%	7.6%

Table 1.

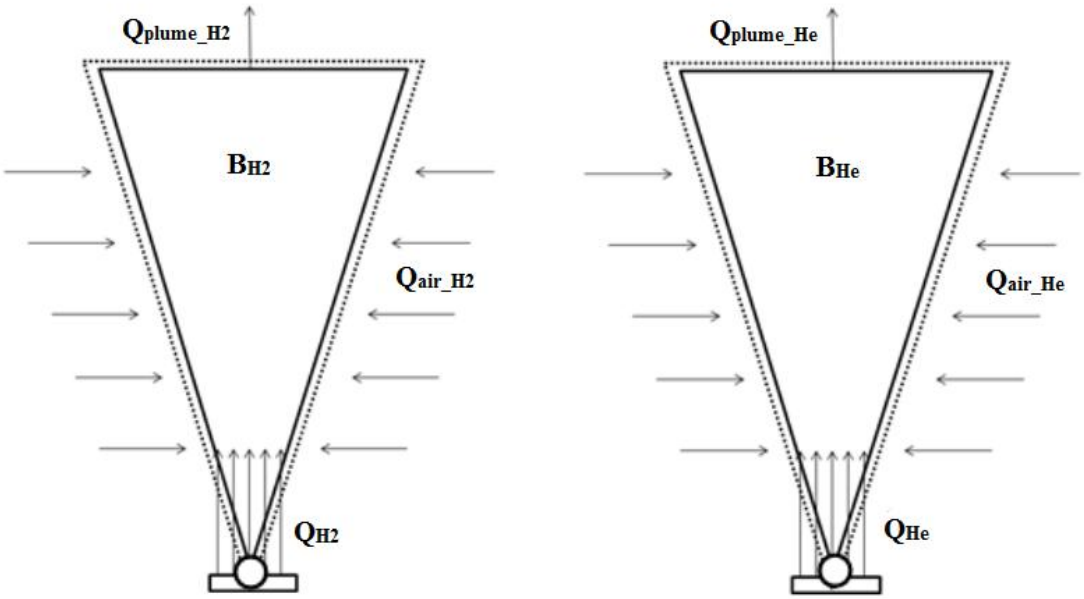

Fig. 1.

(a)

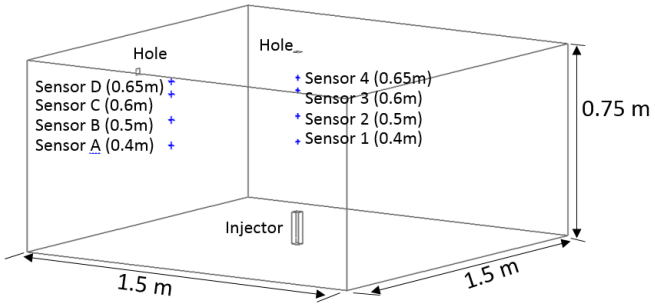
Hole
Hole
Sensor D (0.65m)
Sensor C (0.6m)
Sensor B (0.5m)
Sensor A (0.4m)
Sensor 4 (0.65m)
Sensor 3 (0.6m)
Sensor 2 (0.5m)
Sensor 1 (0.4m)
0.75 m
Injector
1.5 m
1.5 m

(b)

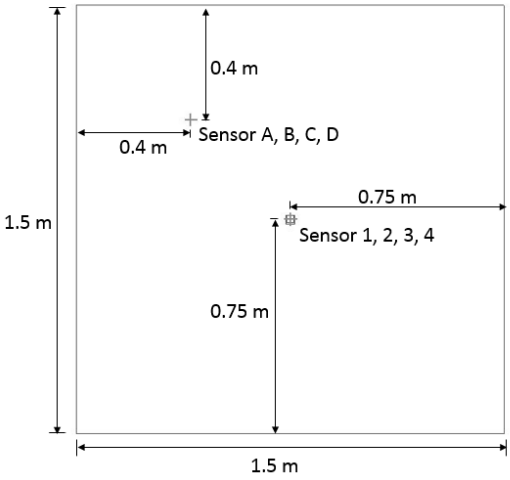
0.4 m
0.4 m
Sensor A, B, C, D
0.75 m
Sensor 1, 2, 3, 4
1.5 m
0.75 m
1.5 m

(c)

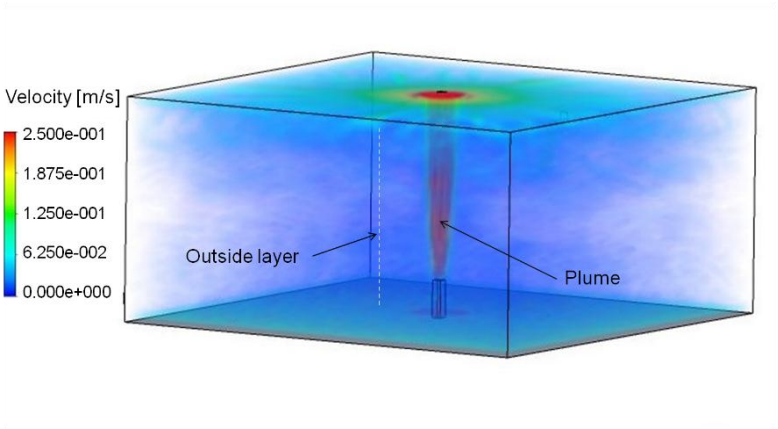
Velocity [m/s]
2.500e-001
1.875e-001
1.250e-001
6.250e-002
0.000e+000
Outside layer
Plume

(d)

Fig. 2.

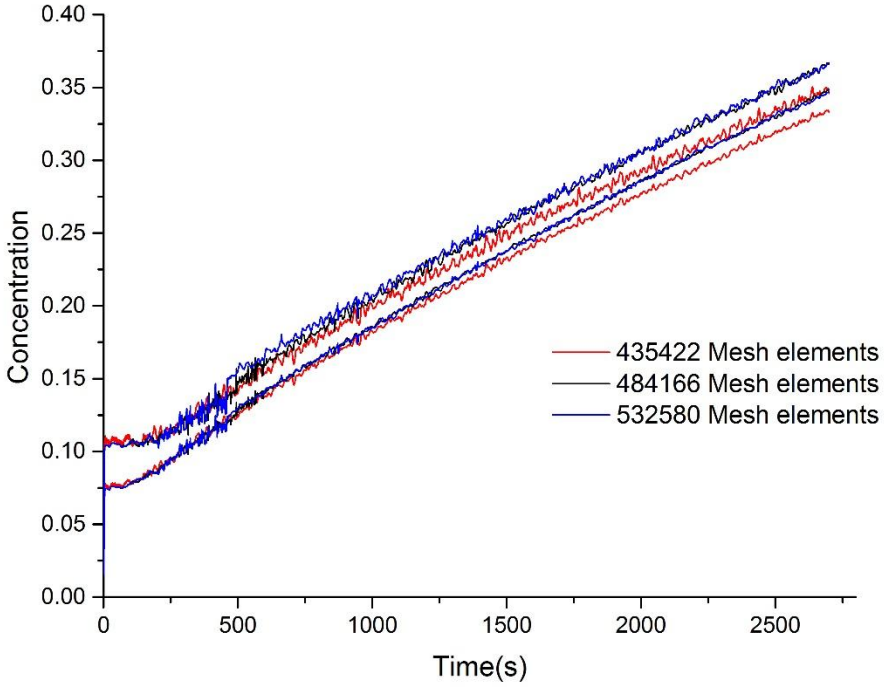
0.40
0.35
0.30
0.25
0.20
0.15
0.10
0.05
0.00
Concentration
0
500
1000
1500
2000
2500
Time(s)
435422 Mesh elements
484166 Mesh elements
532580 Mesh elements

(a)

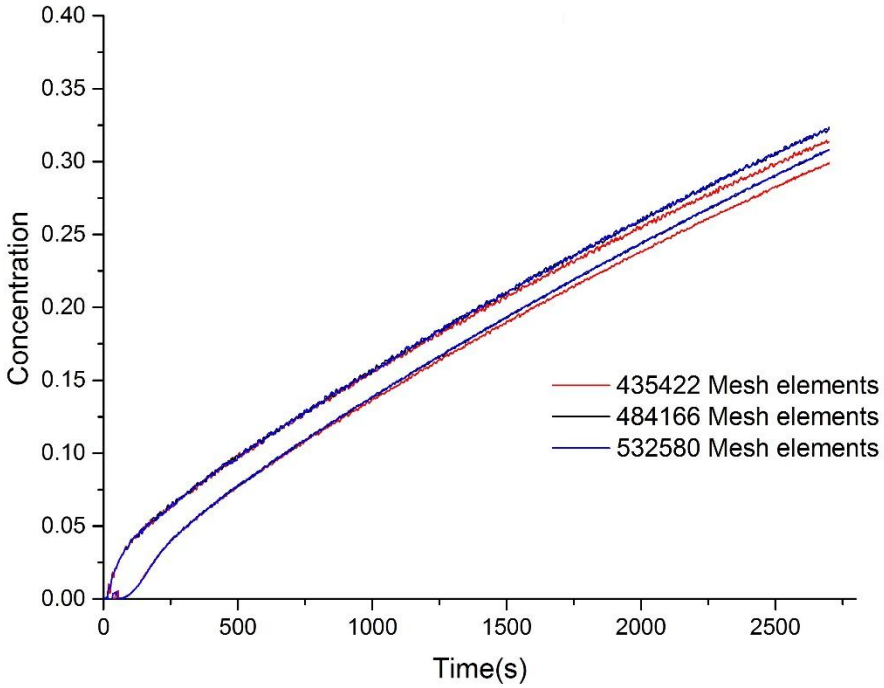
0.40
0.35
0.30
0.25
0.20
0.15
0.10
0.05
0.00
Concentration
0
500
1000
1500
2000
2500
Time(s)
435422 Mesh elements
484166 Mesh elements
532580 Mesh elements

(b)

Fig. 3.

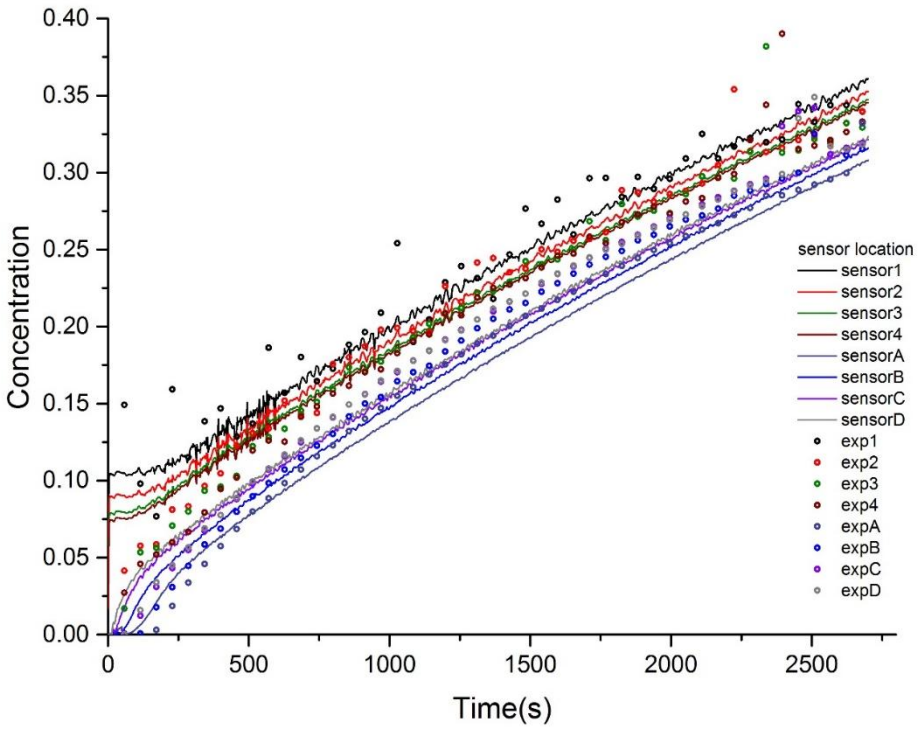
Concentration
Time(s)
0.00
0.05
0.10
0.15
0.20
0.25
0.30
0.35
0.40
0
500
1000
1500
2000
2500
sensor location
sensor1
sensor2
sensor3
sensor4
sensorA
sensorB
sensorC
sensorD
exp1
exp2
exp3
exp4
expA
expB
expC
expD

Fig. 4.

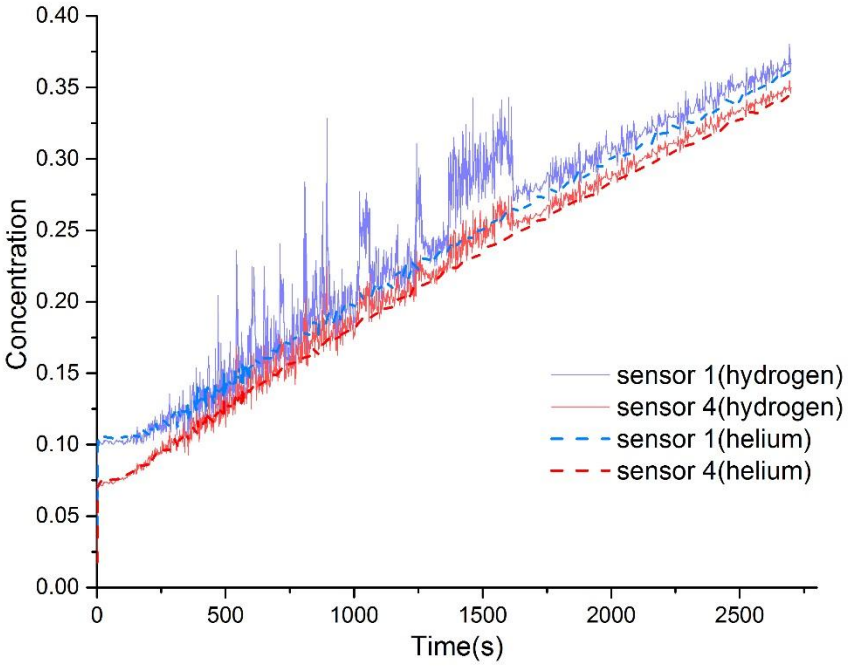

(a)

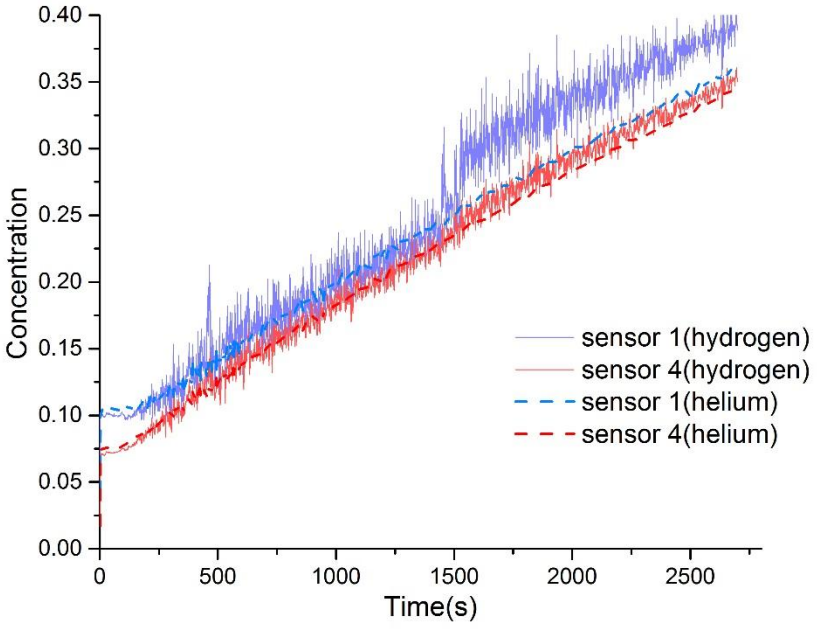

(b)

Fig. 5. (continued)

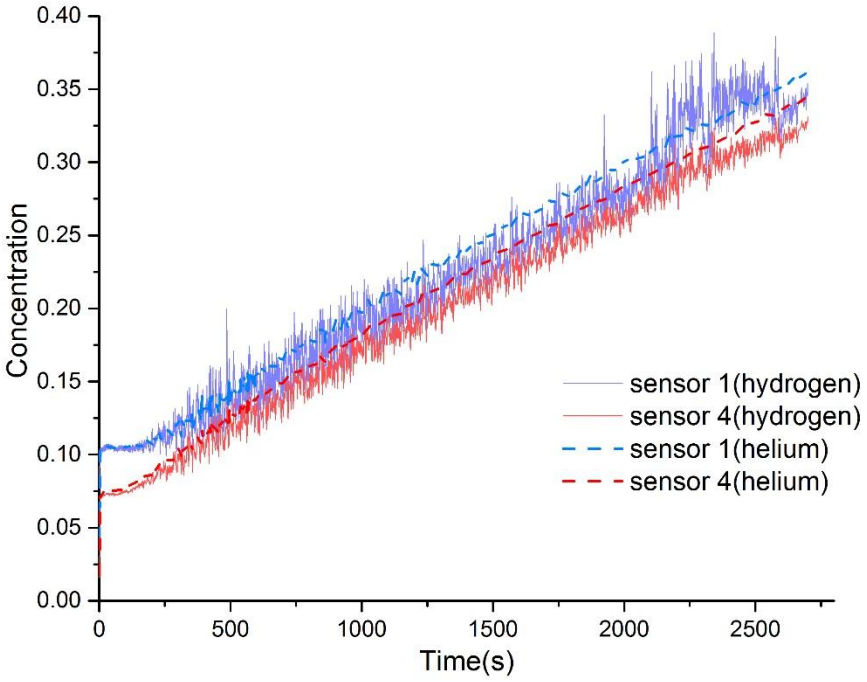
0.40
0.35
0.30
0.25
0.20
0.15
0.10
0.05
0.00
Concentration
0
500
1000
1500
2000
2500
Time(s)
sensor 1(hydrogen)
sensor 4(hydrogen)
sensor 1(helium)
sensor 4(helium)

(c)

Fig. 5.

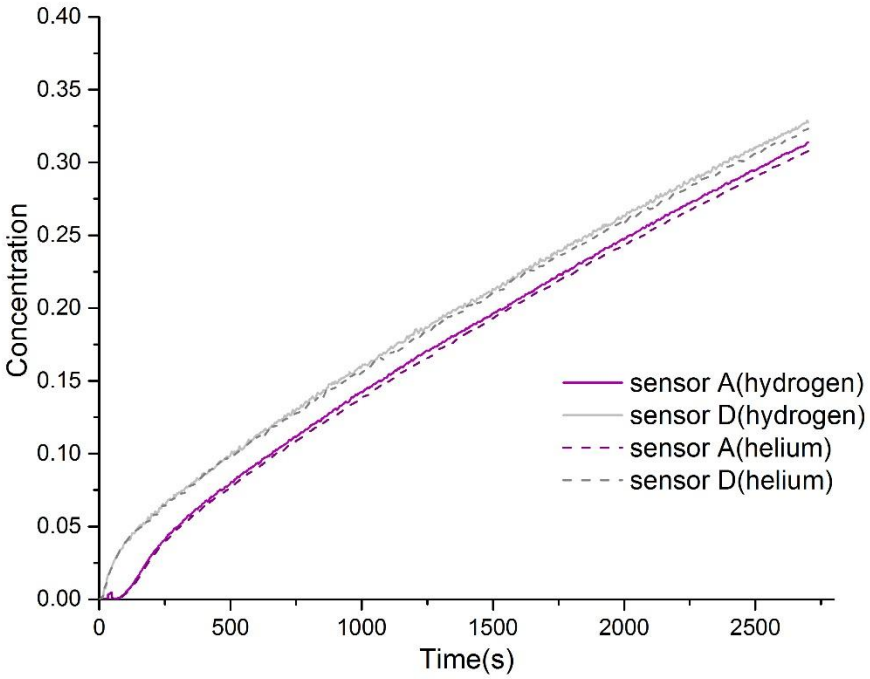

(a)

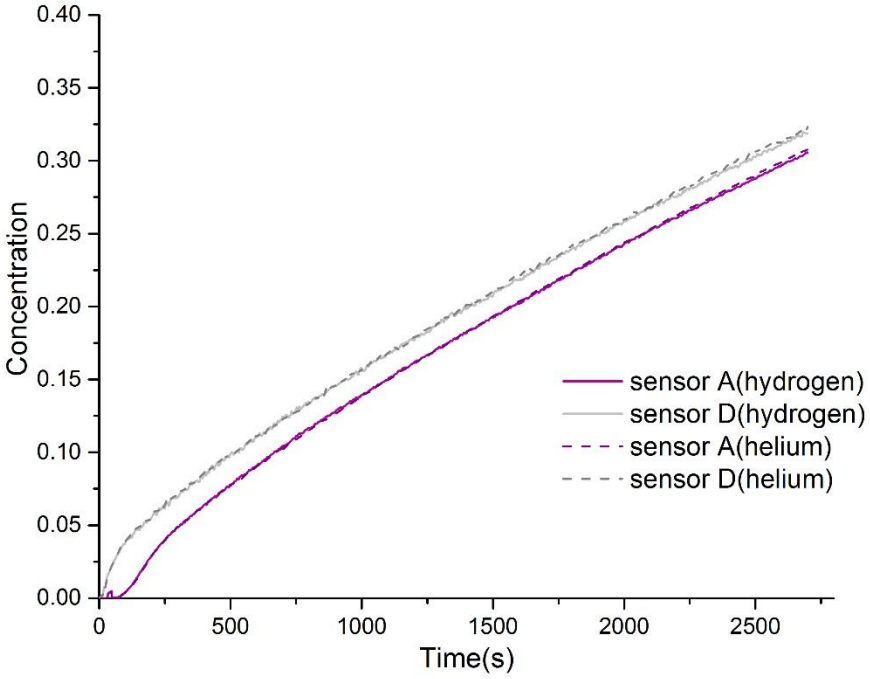

(b)

Fig. 6. (continued)

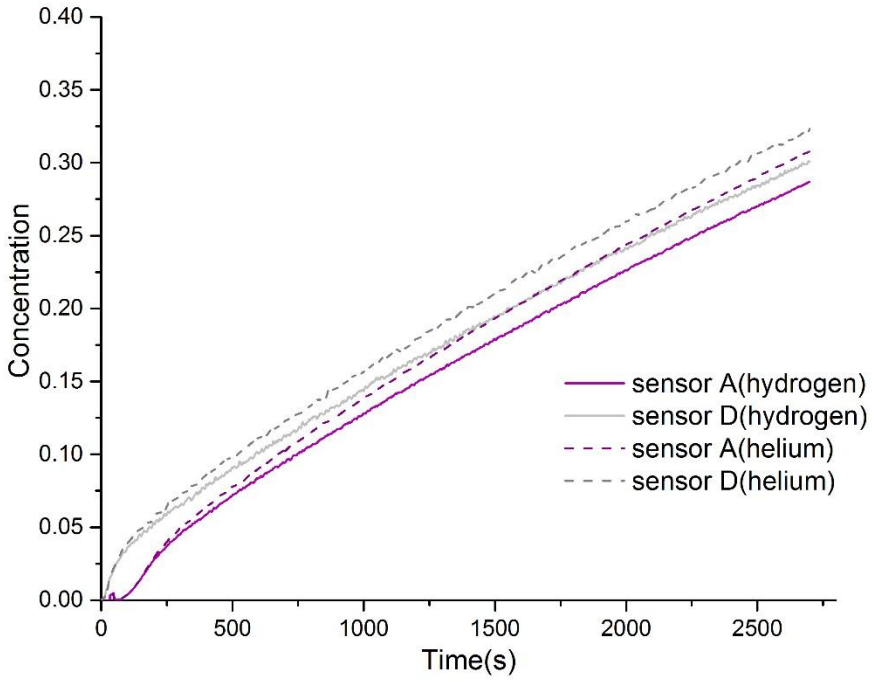
0.40
0.35
0.30
0.25
0.20
0.15
0.10
0.05
0.00
Concentration
0
500
1000
1500
2000
2500
Time(s)
sensor A(hydrogen)
sensor D(hydrogen)
sensor A(helium)
sensor D(helium)

(c)

Fig. 6.

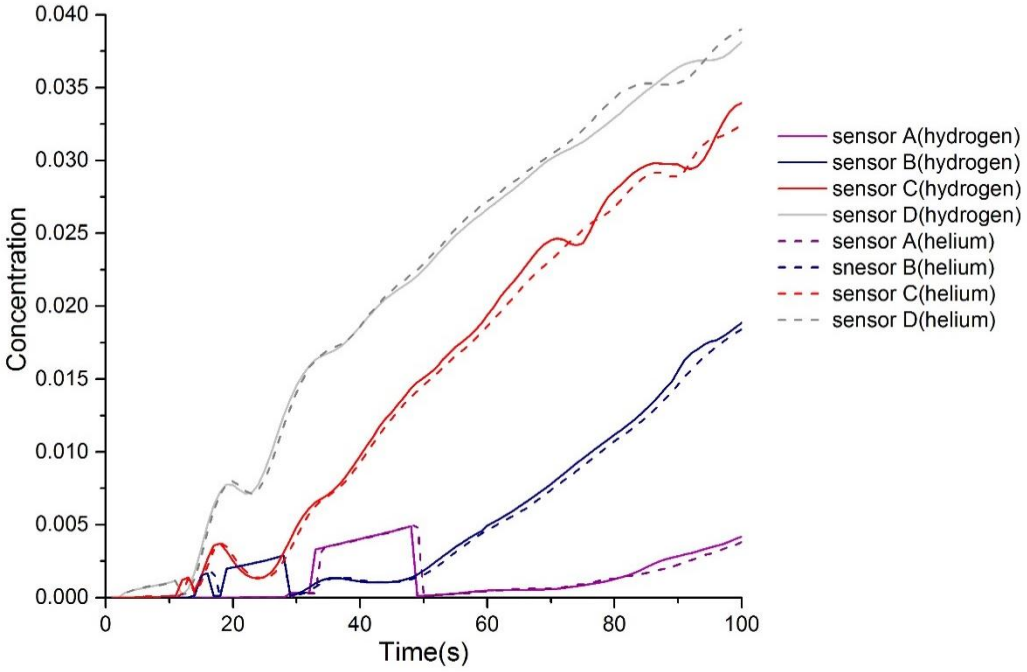

(a)

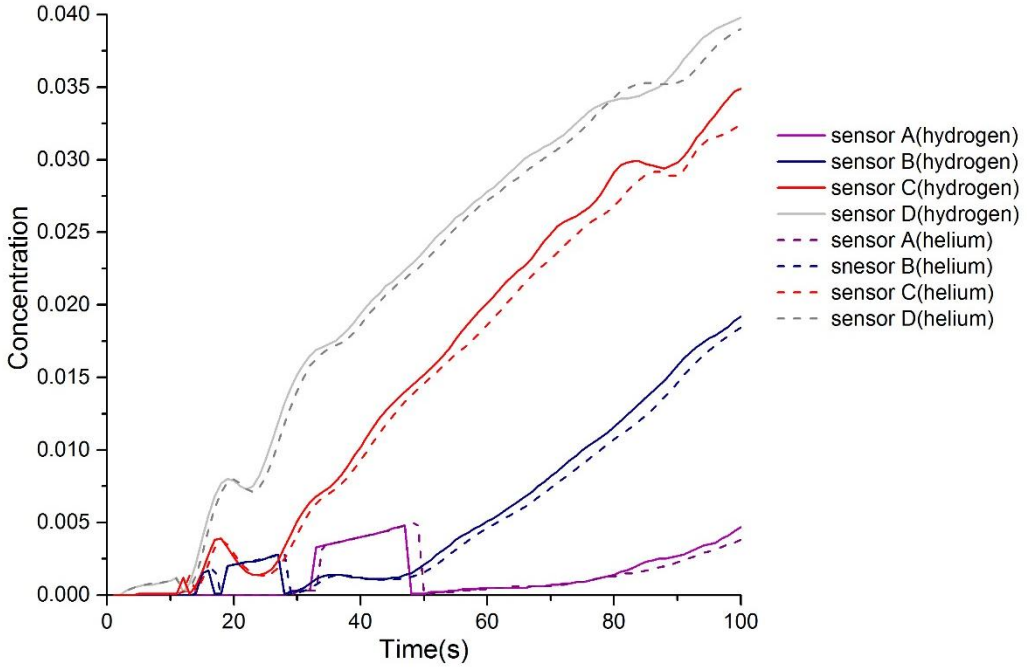

(b)

Fig. 7. (continued)

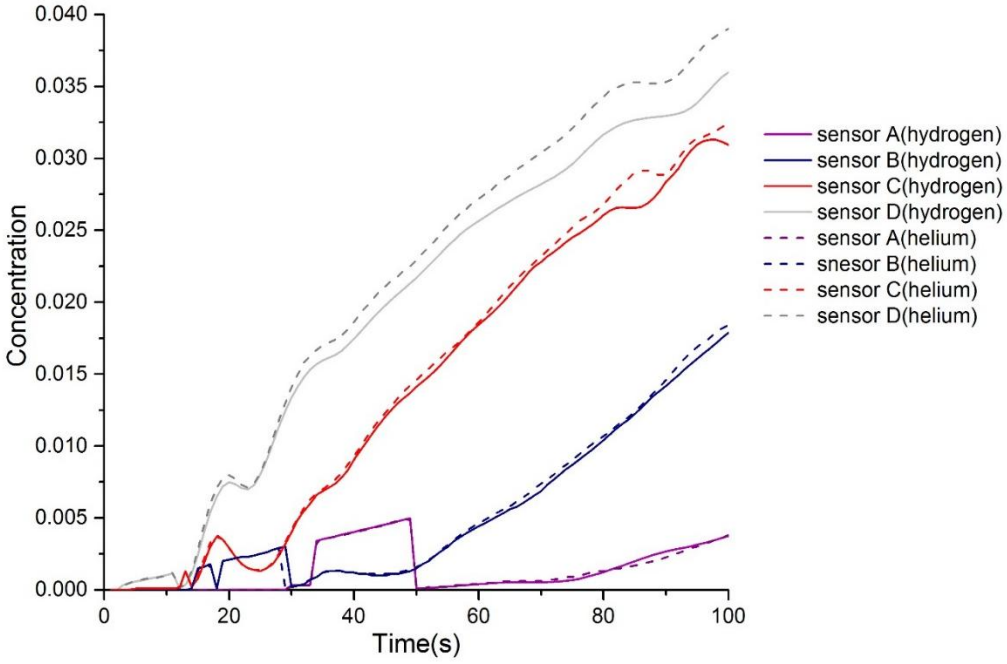
0.040
0.035
0.030
0.025
0.020
0.015
0.010
0.005
0.000
Concentration
0
20
40
60
80
100
Time(s)
sensor A(hydrogen)
sensor B(hydrogen)
sensor C(hydrogen)
sensor D(hydrogen)
sensor A(helium)
snesor B(helium)
sensor C(helium)
sensor D(helium)

(c)

Fig. 7.

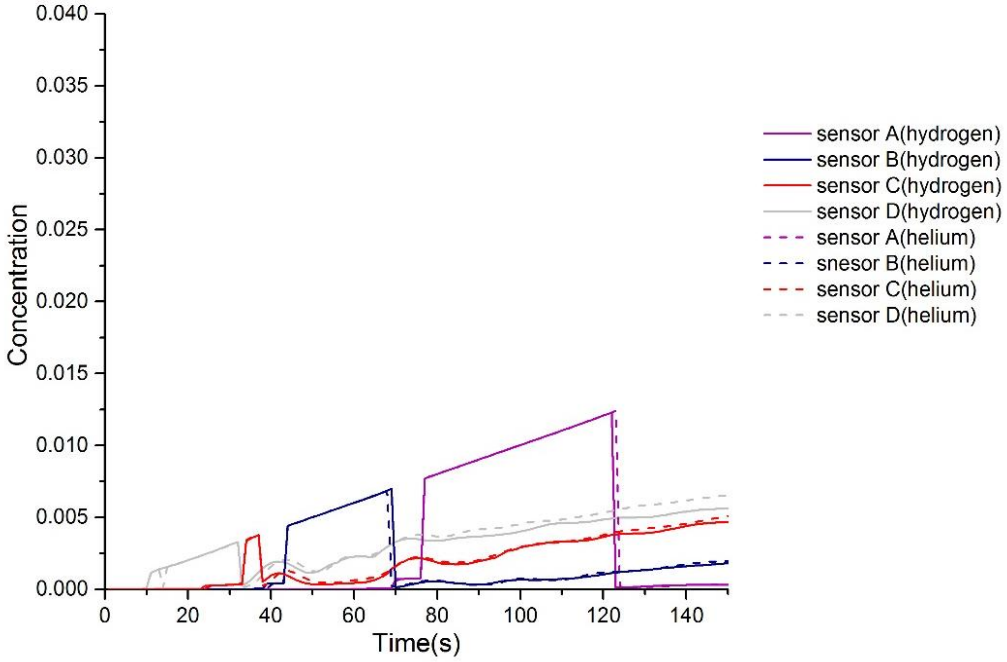

(a)

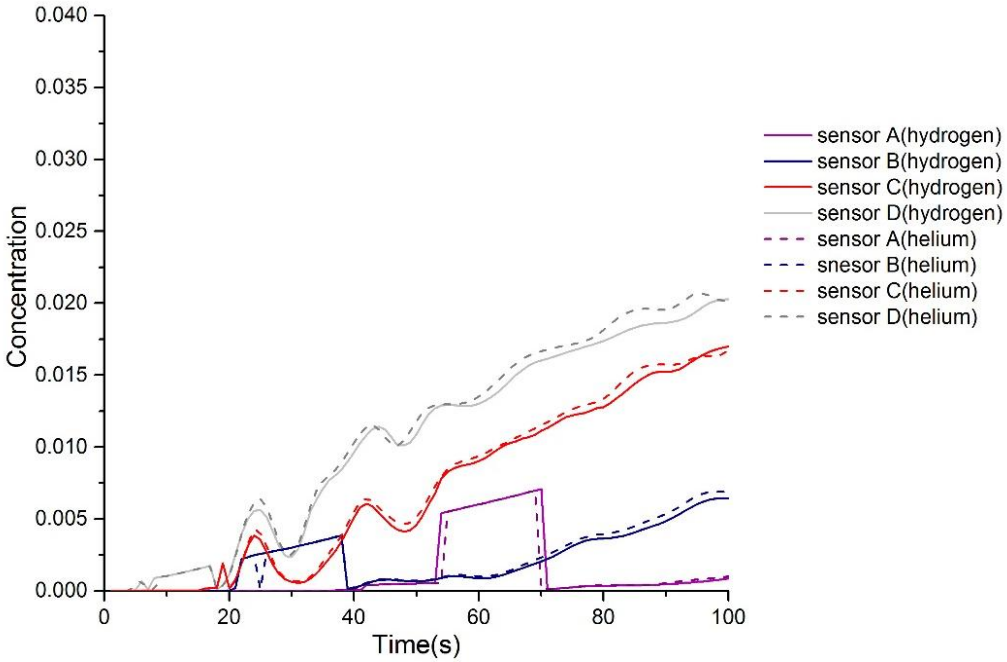

(b)

Fig. 8. (continued)

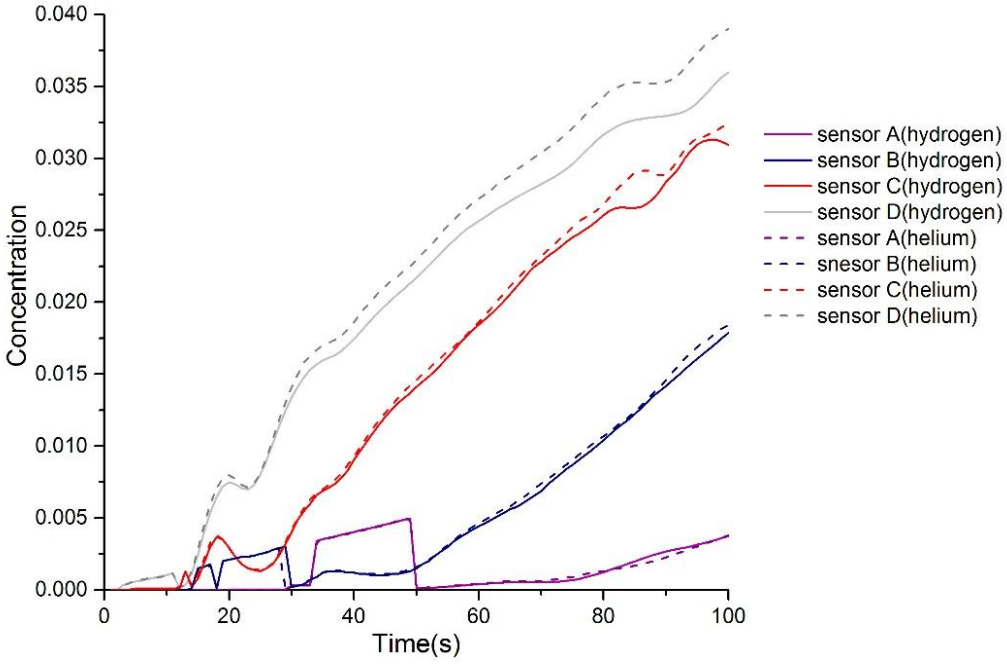
0.040
0.035
0.030
0.025
0.020
0.015
0.010
0.005
0.000
Concentration
0
20
40
60
80
100
Time(s)
sensor A(hydrogen)
sensor B(hydrogen)
sensor C(hydrogen)
sensor D(hydrogen)
sensor A(helium)
snesor B(helium)
sensor C(helium)
sensor D(helium)

(c)

Fig. 8.

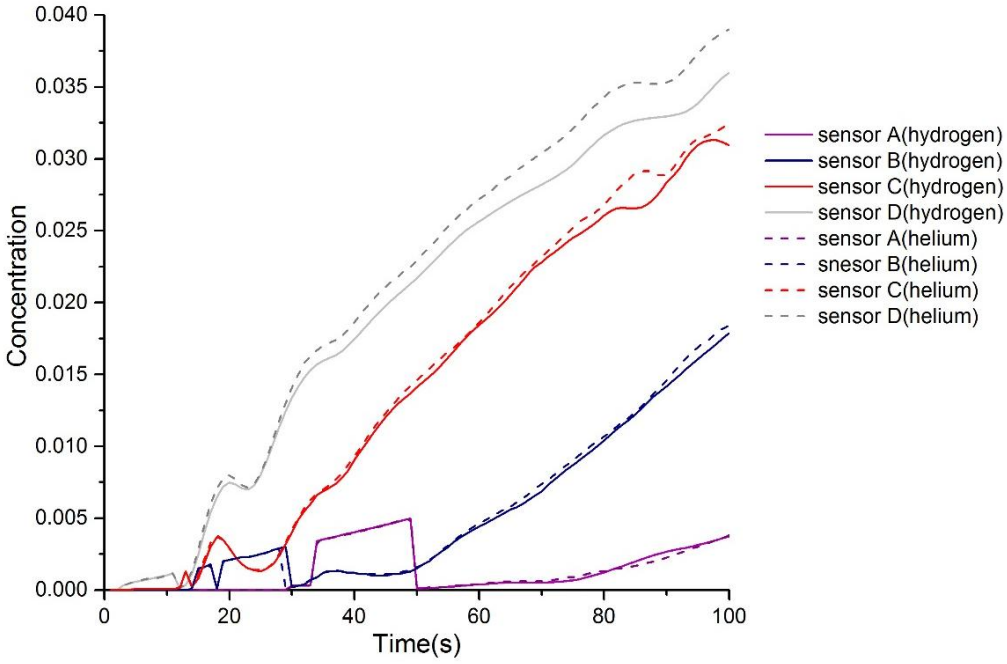

(a)

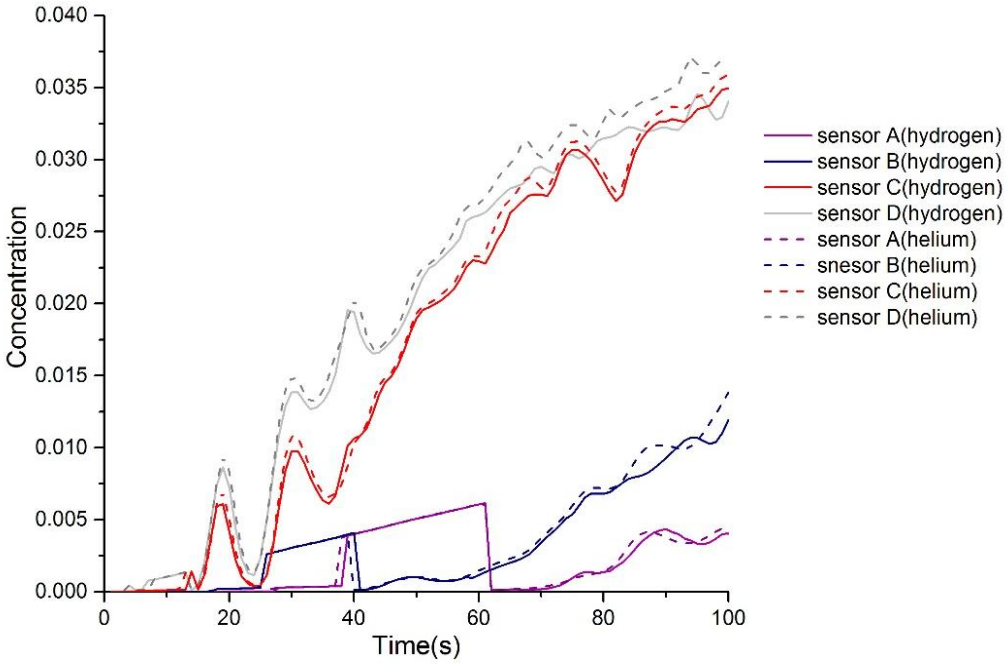

(b)

Fig. 9. (continued)

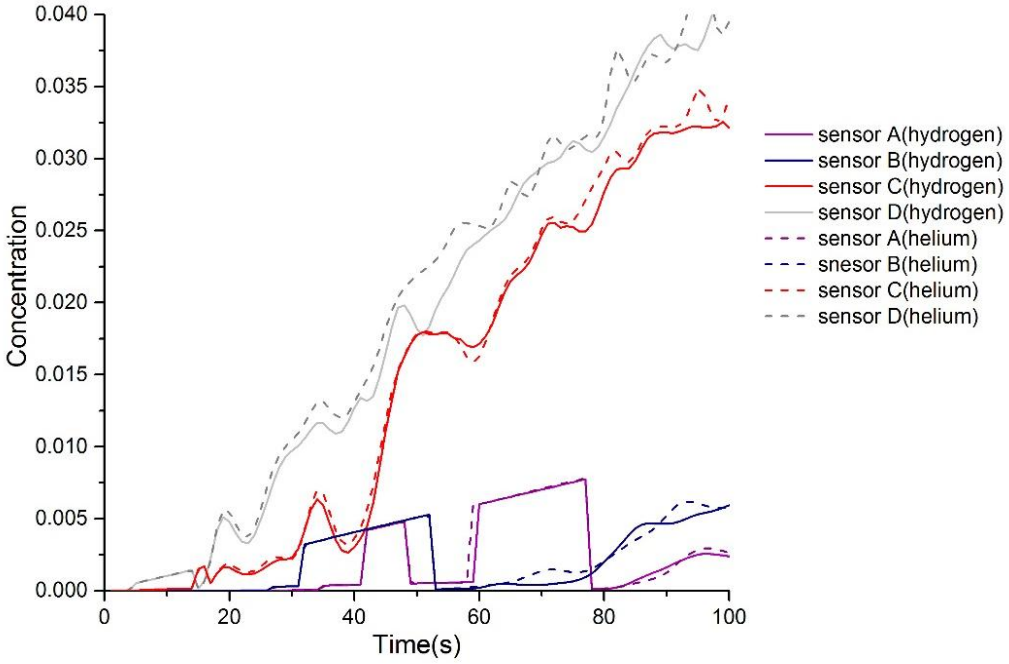
0.040
0.035
0.030
0.025
0.020
0.015
0.010
0.005
0.000
Concentration
0
20
40
60
80
100
Time(s)
sensor A(hydrogen)
sensor B(hydrogen)
sensor C(hydrogen)
sensor D(hydrogen)
sensor A(helium)
snesor B(helium)
sensor C(helium)
sensor D(helium)

(c)

Fig. 9.

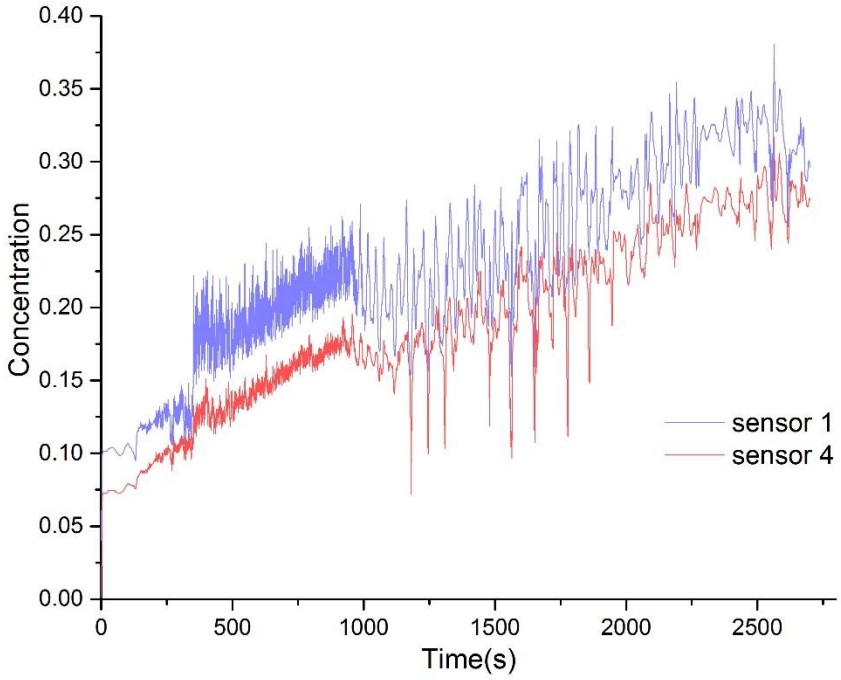
0.40
0.35
0.30
0.25
0.20
0.15
0.10
0.05
0.00
Concentration
0
500
1000
1500
2000
2500
Time(s)
sensor 1
sensor 4

Fig. 10.

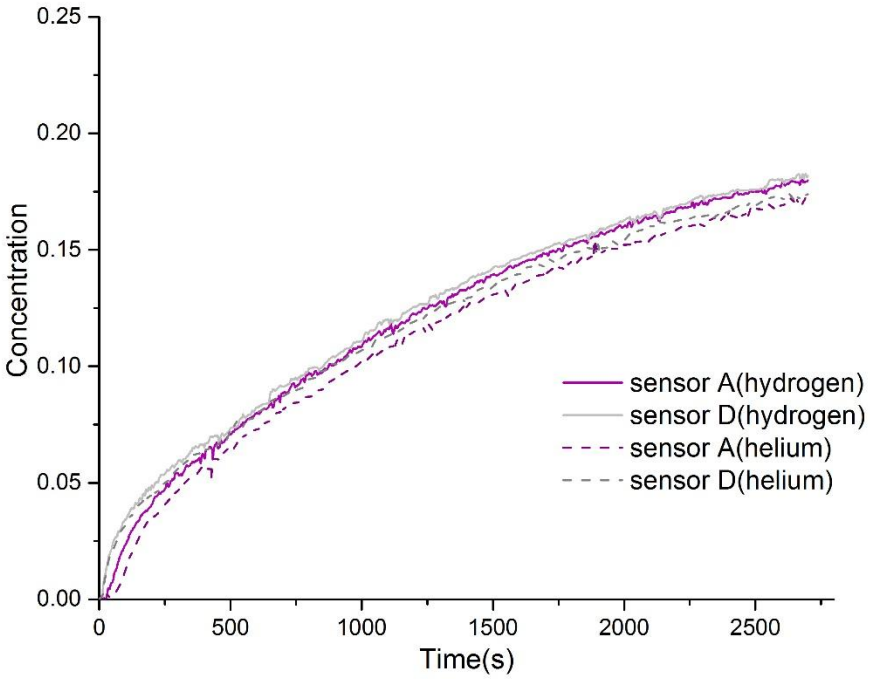

(a)

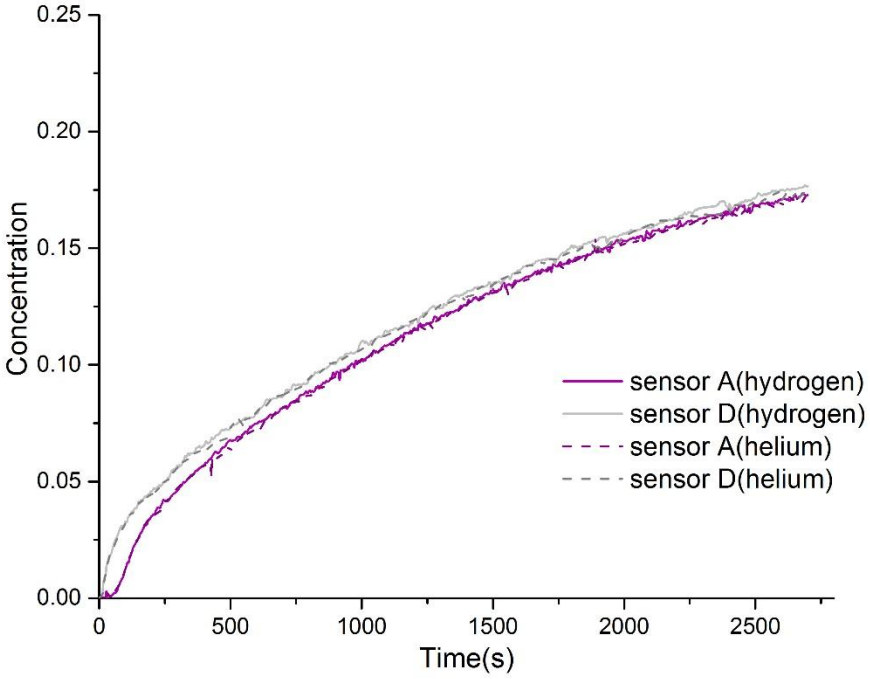

(b)

Fig. 11. (continued)

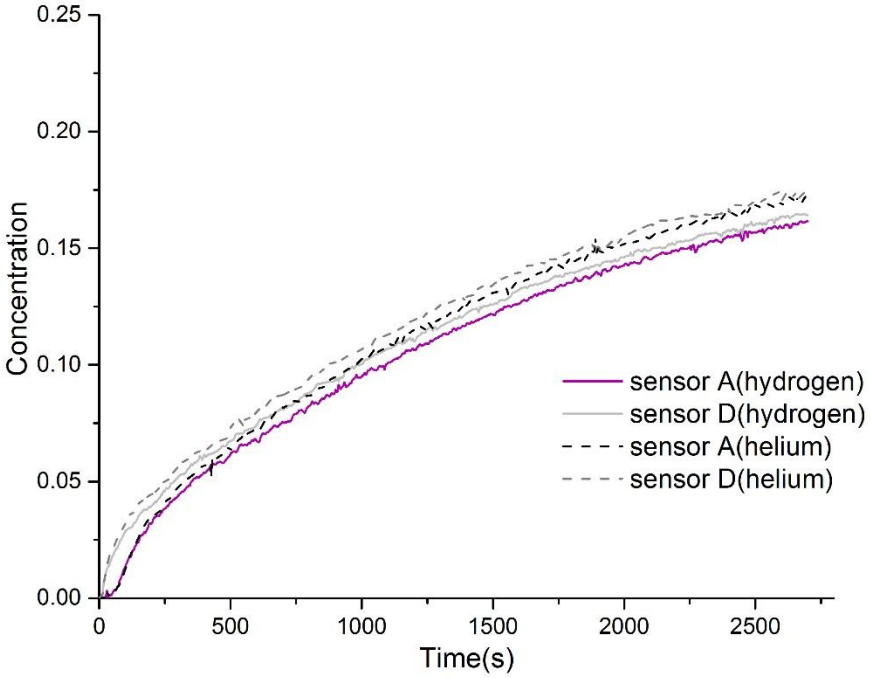
0.25
0.20
0.15
0.10
0.05
0.00
Concentration
0
500
1000
1500
2000
2500
Time(s)
sensor A(hydrogen)
sensor D(hydrogen)
sensor A(helium)
sensor D(helium)

(c)

Fig. 11.

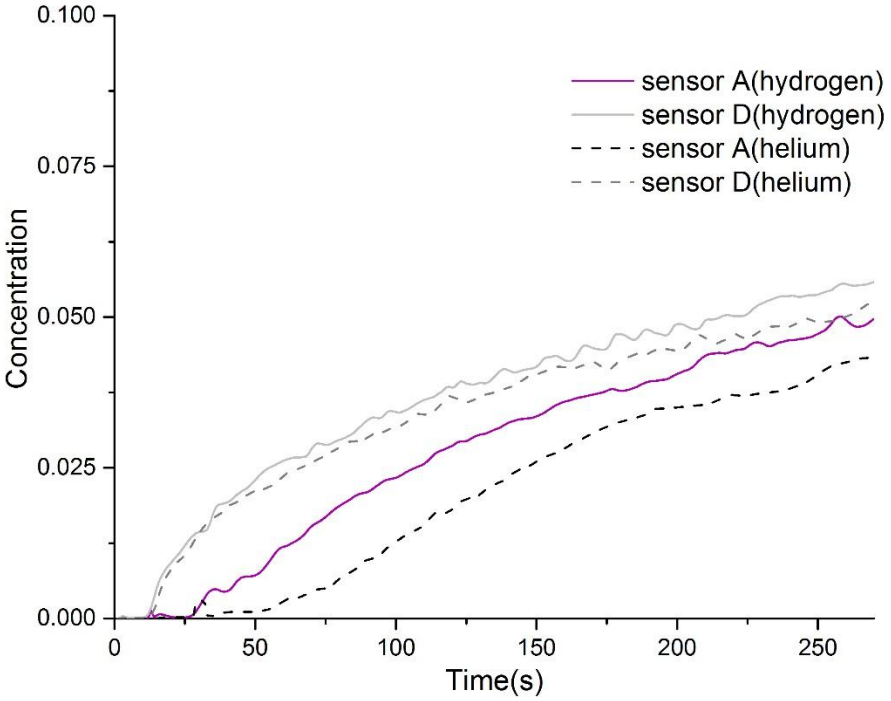

(a)

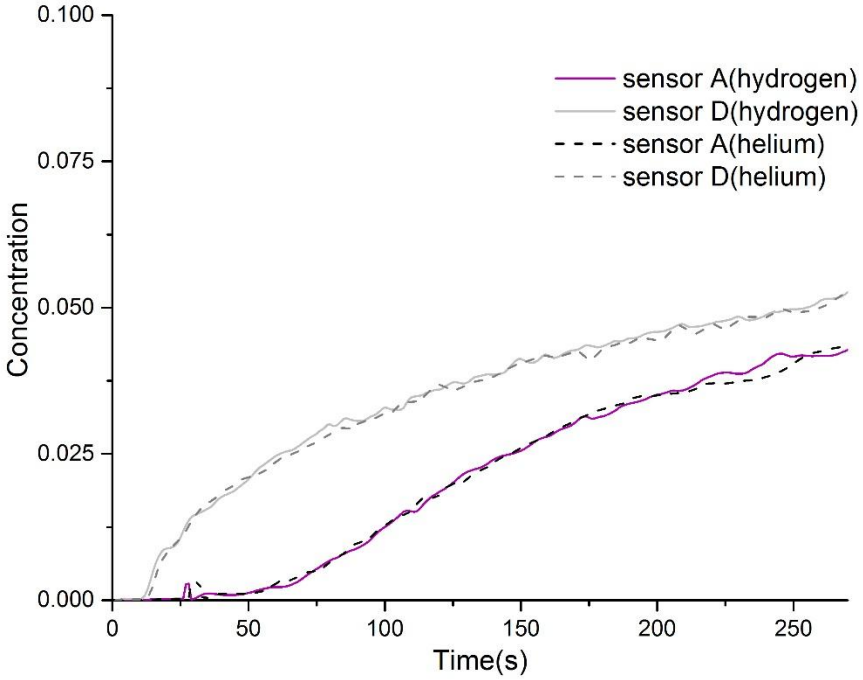

(b)

Fig. 12. (continued)

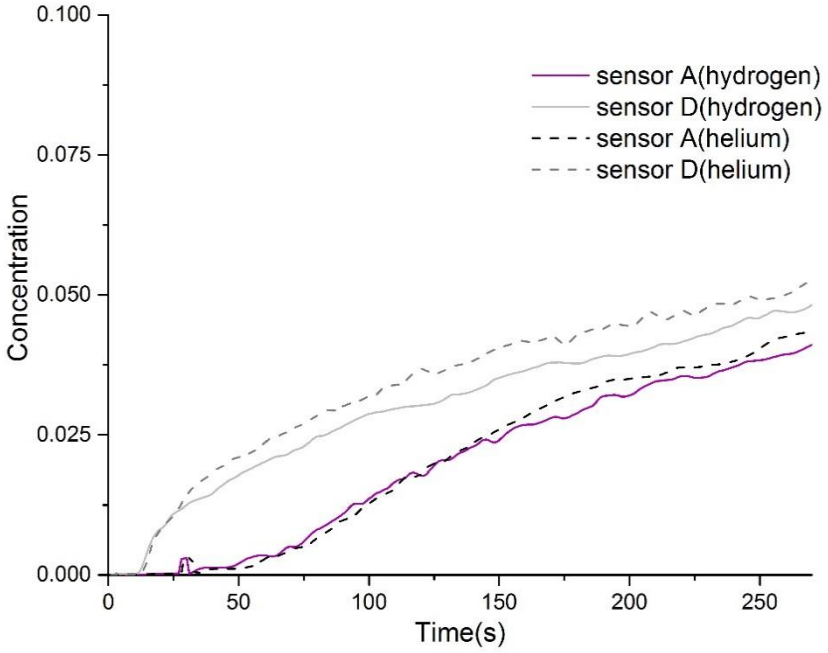
0.100
0.075
0.050
0.025
0.000
Concentration
0
50
100
150
200
250
Time(s)
sensor A(hydrogen)
sensor D(hydrogen)
sensor A(helium)
sensor D(helium)

(c)

Fig. 12.